



Effect of Two Baffles on MHD Natural Convection in U-Shape Superposed by Solid Nanoparticle having Different Shapes

Hameed K. Hamzah¹, Farooq H. Ali¹, M. Hatami², D. Jing²

¹ College of Engineering-Mechanical Engineering Department, University of Babylon, Babylon City-Hilla, Iraq

² International Research Center for Renewable Energy, State Key Laboratory of Multiphase Flow in Power Engineering, Xi'an Jiaotong University, Xi'an 710049, China

Received March 27 2020; Revised June 22 2020; Accepted for publication June 29 2020.

Corresponding author: M. Hatami (m.hatami@xjtu.edu.cn)

© 2020 Published by Shahid Chamran University of Ahvaz

Abstract. In this paper, numerical Galerkin Finite Element Method (GFEM) applies for natural convection heat transfer of U-shaped cavity filled by Fe₃O₄-water nanofluid under the magnetic field and including two baffles. The above boundaries of the cavity are at low temperatures and bottom boundary is in a variable function temperature. It is assumed that two baffles in the cavity make vortices to enhance heat transfers. The dimensionless governing equations including velocity, pressure, and temperature formulation are solved by the Galerkin finite element method. The results are discussed based on the governing parameters such as a nanoparticle volume fraction, Hartmann and Rayleigh numbers, magnetic field angle and nanoparticles shapes. As a main result, increasing both Aspect Ratio (AR) and Ra numbers enhanced heat transfer process and improved the average Nusselt numbers, while increasing the Hartmann number decreased the Nusselt number. Furthermore, it concluded that AR=0.4 had the maximum ψ and Nusselt numbers among the other examined aspect ratios. Also, platelet, cylindrical, brick and spherical shapes had the maximum Nusselt numbers in sequence.

Keywords: Baffle; Nusselt Number; Natural Convection; Magnetic Field; GFEM.

1. Introduction

Baffles are devices which makes changes the flow patterns and makes more vortex or turbulence in the flow, so they have a large applications in heat transfer devices such as heat exchangers in industries. Recently, Ma et al. [1] applied the Lattice Boltzmann method (LBM) to find the nanofluid natural convection behavior in a baffled U-shaped cavity in the existence of a magnetic field. They found that the average Nusselt number increased by growths the Rayleigh number, nanoparticle solid volume fraction and aspect ratio. Abedini et al. [2] investigated the influence of a baffle for a water-Fe₃O₄ nanofluid on free convection heat transfer in a C-shaped cavity in the existence of a magnetic field using control volume method. They reported that growing the baffle length makes improvements in the Nusselt number where the maximum cooling process was occurred when AR=0.7. In another study on the C-shaped cavities, Aghakhani et al. [3] applied the finite difference lattice Boltzmann method in a non-Newtonian and power-law fluid under a magnetic field (as external force) inside a C-shaped enclosure and reported that Nusselt number declines by increasing power-law index (n) at larger Rayleigh numbers. Also, they found that an increase in the Hartmann number makes a reduction in heat transfer rate. Hussain et al. [4] used the finite volume method for air heat transfer in a sinusoidal corrugated enclosure and investigated the effect of corrugation frequency and Rayleigh numbers on the Nusselt number. In another study on the corrugated enclosure, Salam et al. [5] investigated the effect of inclination angle on the heat transfer in a sinusoidal enclosure and discussed on the Nusselt number results. Also, Farooq Hassan Ali [6] studied the natural convection in an sloping enclosure contained silver-water nanofluid and reported that important shaping wall and high concentration of Ag-nanoparticles are effective ways to enhance the heat transfer rate. Abu-Nada and Hakan Oztop [7] investigated the inclination angle of geometry on the natural convection heat transfer on Cu-water nanofluid. Abdulkadhim et al. [8] studied the entropy generation caused by thin baffle in a trapezoidal cavity filled by nanofluid and found that when Rayleigh number increases, fluid flow strength were improved and heat transfer were enhanced. A complete review of entropy generation due to nanofluids application is presented by Omid et al. [9].

Nanofluids which are made from the different phases (fluid-solid) has many applications in heat transfer due to different thermal conductivity and other thermo-physical properties compared to based fluid. Hatami and Ganji [10-11] investigated the particle motion (as the solid phase) in forced vortex and rotating parabola using DQM and DTM. Also, Dogonchi et al. [12] and Hatami et al. [13] investigated the particles motion in Couette flow using different and new analytical techniques such as multi-step differential transformation method (Ms-DTM). Recently, most of the researchers in the field of nanofluid, were motivated to do their studies by the efficient numerical techniques to reduce the costs. Ghadikolaei et al. [14] considered Fe₃O₄-(CH₂OH)₂ nanofluid in a porous medium under MHD field using analytical methods. Hatami et al. [15] numerically optimized the circular-



wavy cavity using finite element method and response surface methodology. Hatami [16] used the same numerical method to find the nanoparticles migration around the heated cylinder in a wavy-wall enclosure. Tang et al. [17], based on two last studies, optimized the geometry of cavity include double sinusoidal wavy walls to find the best heat transfer efficiency.

Some applications of nanofluids are presented by the researchers such as Hatami and Jing [18] which used them for the wavy direct absorber solar collector (WDASC) and optimized the proposed geometry with the introduced numerical methods. Also, Hatami et al. [19] used the same procedures for a lid-driven T-shaped porous media and improved the mixed convection heat transfer. In another application study, Zhou et al. [20] used the RSM and FVM for designing the microchannel heat sink with wavy channel. Kefayati [21-22] used the numerical methods for the entropy generation of MHD nanofluid for non-Newtonian and Bingham fluid, respectively. Also, Kefayati and Tang [23] used the Buongiorno's mathematical model for the entropy generation of MHD non-Newtonian nanofluid in a cavity. Menni et al. [24] reviewed the recent studies on the solar collectors using nanofluids and Kefayati et al. [25-28] investigated the effect of nanofluids in different cavity geometries as an applicable studies for the solar collector's applications. Mehryan et al. [29] and Dogonchi et al. [30-31] also studied the natural and free convection heat transfer of nanofluids in presence of magnetic field. Furthermore, MHD effect of Casson nanofluid is studied by Shah et al. [32] and Alsabery et al. [33]. Dinarvand et al. [34] and Alsabery et al. [35] also considered the effect of nanofluid heat transfer over a moving wedge and porous medium, respectively.

Based on above short review, in this paper, it is aimed to use the Galerkin Finite Element Method (GFEM) for natural convection heat transfer of U-shaped cavity filled by Fe3O4-water nanofluid under the magnetic field and including two baffles. The effect of some appeared parameters, aspect ratio for the baffles and nanoparticles shapes on the average Nusselt numbers are discussed in this manuscript.

2. Physical Model Description and Governing Equations

U-shaped cavities have a large application in solar energy industry [24], microchannels, automobile radiators, etc. In this study a U-shaped cavity including baffles and fins as found in cross-section of solar collectors (Fig. 1) is considered. The schematic plan of this U-geometry enclosure with two baffles in each corner of the cold fin as described in Fig. 1a. The length of the enclosure with X-axis indicated by (W) and with Y-axis by (H). The dimensions of the cold square fin is (L), there are two baffles on each corner of the cold square fin with length equal to (h).

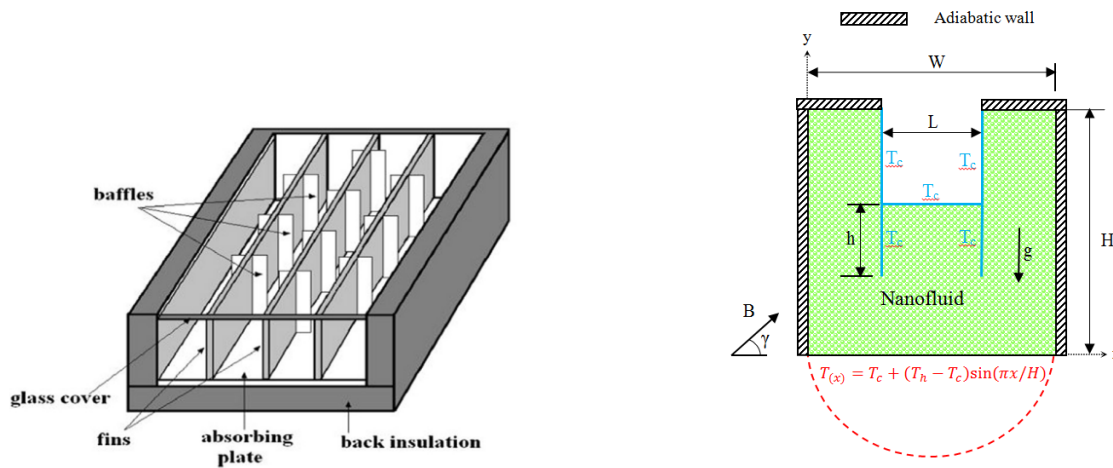


Fig. 1a. Fins and baffles in solar collector application [24] (left), Schematic diagram of the present problem (right)

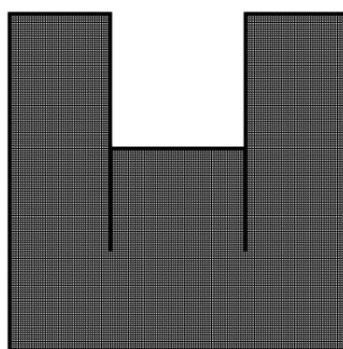


Fig. 1b. Mesh distribution of the present problem

Table 1. Properties of base fluids and nanoparticles

Material/Properties	ρ (kg/m ³)	C_p (J/kg-K)	k (W/m-K)	μ (kg/m-s)	σ (μ S/cm)
Water	997.1	4179	0.613	0.0010003	0.05
Fe ₃ O ₄	5200	670	6	-	25000



The relations between dimensions of the enclosure are $W=1$, $H/W=1$, $h/W=0.3$, and aspect ratio ($AR=L/H$) is taken equal to 0.2, 0.4 and 0.6. The enclosure filled with water superposed by Fe₃O₄ nanoparticles having four different shapes of solid nanoparticles. The nanoparticles shape (λ) and thermo-physical properties of Fe₃O₄ nanofluid are titled in table (1). The bottom wall of the enclosure was kept at $T(X) = T_c + (T_h - T_c)\sin(\pi X/H)$ hot temperature. The top wall was kept at a constant cold temperature (T_c) while the rest walls are adiabatic [3].

In this work, steady, laminar, incompressible, two-dimensional, Newtonian fluid are supposed and viscous dissipation is neglected and induced magnetic field assumed to be negligible compared to external magnetic field. Thermo-physical properties of Fe₃O₄-water nanofluid are supposed to be constant except the density, which variation with temperature and is modeled with a Boussinesq approach. Magnetic field with variable orientation angle (γ) is considered with uniform distribution ($\vec{B}_0 = B_{0x}e_x + B_{0y}e_y$) where e_x and e_y are vector unity. After this assumption, the differential equations are described the fluid flow and heat transfer are continuity, momentum and energy. The dimensionless form of these equations in Cartesian coordinates are:

Continuity equation [1-2]:

$$\frac{\partial U}{\partial X} + \frac{\partial V}{\partial Y} = 0 \quad (1)$$

Momentum equation in X-direction

$$U \frac{\partial U}{\partial X} + V \frac{\partial U}{\partial Y} = -\frac{\partial P}{\partial X} + \frac{\mu_{na}}{\rho_{na}\alpha_{bf}} \left(\frac{\partial^2 U}{\partial X^2} + \frac{\partial^2 U}{\partial Y^2} \right) + Ha^2 \left(\frac{\rho_{na}}{\rho_{bf}} \right) \left(\frac{\sigma_{na}}{\sigma_{bf}} \right) (V \sin \gamma \cos \gamma - U \sin^2 \gamma) \quad (2)$$

Momentum equation in Y-direction

$$U \frac{\partial V}{\partial X} + V \frac{\partial V}{\partial Y} = -\frac{\partial P}{\partial Y} + \frac{\mu_{na}}{\rho_{na}\alpha_{bf}} \left(\frac{\partial^2 V}{\partial X^2} + \frac{\partial^2 V}{\partial Y^2} \right) + \left(\frac{\rho\beta}{\rho\beta} \right)_{na} Ra Pr \theta + Ha^2 Pr \left(\frac{\rho_{bf}}{\rho_{na}} \right) \left(\frac{\sigma_{na}}{\sigma_{bf}} \right) (U \sin \gamma \cos \gamma - V \cos^2 \gamma) \quad (3)$$

Energy equation

$$U \frac{\partial \theta}{\partial X} + V \frac{\partial \theta}{\partial Y} = \frac{\alpha_{na}}{\alpha_{bf}} \left(\frac{\partial^2 \theta}{\partial X^2} + \frac{\partial^2 \theta}{\partial Y^2} \right) \quad (4)$$

Following dimensionless parameter and numbers were assumed to obtain above governing equations [1-2]:

$$X, Y = \frac{x, y}{H}; U, V = \frac{(u, v)H}{\alpha_{bf}}; \theta = \frac{(T - T_c)}{(T_h - T_c)}; Pr = \frac{\nu_{bf}}{\alpha_{bf}} \quad (5)$$

$$Ra = \frac{g\beta_{bf}H^3(T_h - T_c)}{\alpha_{bf}\nu_{bf}}; P = \frac{\rho H}{\rho_{na}\alpha_{bf}^2}; Ha = B_0 H \sqrt{\frac{\sigma_{na}}{\rho_{na}\nu_{na}}}$$

The thermo-physical properties of the Fe₃O₄ nanoparticles employed in this study are explained in the following relations [18-19]:

Density:

$$\rho_{na} = (1 - \phi)\rho_{bf} + \phi\rho_{sp} \quad (6)$$

where (ϕ) specified solid nanoparticles volume fraction.

Specific heat:

The specific heat of the mixture water-nanofluid was calculated as:

$$(\rho c_p)_{na} = (1 - \phi)(\rho c_p)_{bf} + \phi(\rho c_p)_{sp} \quad (7)$$

Thermal expansion:

The coefficient of thermal expansion for water-nanofluid was specified by the following relation:

$$(\rho\beta)_{na} = (1 - \phi)(\rho\beta)_{bf} + \phi(\rho\beta)_{sp} \quad (8)$$

Electrical conductivity

The ratio of Fe₃O₄ nanoparticles electrical conductivity to the base fluid (water) electric conductivity described by the following equation:

$$\frac{\sigma_{na}}{\sigma_{bf}} = 1 + \frac{3\phi \left(\frac{\sigma_{sp}}{\sigma_{bf}} - 1 \right)}{\left(\frac{\sigma_{sp}}{\sigma_{bf}} + 2 \right) - \left(\frac{\sigma_{sp}}{\sigma_{bf}} - 1 \right) \phi} \quad (9)$$

Thermal conductivity:

Thermal conductivity effectiveness of the liquid phase (water) and solid phase (Fe₃O₄) nanoparticles was defined by the following equation introduced by Hamilton and Crosser [36]:

$$\frac{k_{na}}{k_{bf}} = \frac{k_{sp} + (m - 1)k_{bf} - (m - 1)\phi(k_{bf} - k_{sp})}{k_{sp} + (m - 1)k_{bf} + \phi(k_{bf} - k_{sp})} \quad (10)$$



Table 2. Constant of Eq. (11)

Nanoparticle Shape	λ
Spherical	1
Platelet	0.52
Cylindrical	0.62
Brick	0.81

Table 3. Grid independence test for Average Nusselt number and $|\Psi|_{\max}$ on hot surface, AR=0.4, Ra=10⁶, $\lambda=0.52$, $\phi=0.05$, Ha=60, $\nu=90$

Grid size	Nu_{ave}	$\Delta = \frac{ Nu_{i,j} - Nu_{150 \times 150} }{Nu_{i,j}} \times 100$	$ \Psi _{\max}$	$\Delta = \frac{ \Psi_{i,j} - \Psi_{150 \times 150} }{\Psi_{i,j}} \times 100$
100x100	6.7264	1.0303	8.6266	0.43934
150x150	6.7957	-	8.6645	-
200x200	6.8226	0.39428	8.6769	0.14291
250x250	6.8362	0.59243	8.6824	0.20616
300x300	6.8441	0.70718	8.6840	0.22455

Table 4. Nu_{ave} , Ra=1e5, $\phi=0.05$, Ha=20, AR=0.4

Ha	Present study	Yuan Ma et al.[2019]	Error %
0	9.112	9	-1.244
20	7.435	7.45	-0.201
40	4.454	4.5	1.0222
60	3.010	3	-0.333

In the above equation, m refers the shape factor and obtained from the following relation:

$$m = \frac{3}{\lambda} \quad (11)$$

where λ represents nanoparticles shape, as expressed in a Table (2).

Viscosity:

The effective viscosity relation of the mixture water-nanofluid is given by:

$$\mu_{na} = \frac{\mu_{bf}}{(1 - \phi)^{2.5}} \quad (12)$$

The velocity and thermal boundary conditions of the current study work are no-movement and no-diffusion conditions for each wall of the enclosure ($U=V=0$). Bottom wall thermal boundary condition is sinusoidal temperature distribution, cold temperature was applied to the top wall and baffles ($\theta=0$) and two vertical walls are adiabatic ($\partial\theta / \partial X = 0$) _{$X=0,1$} .

The flow field is defined by streamfunction plots which expressed by the two equations below:

$$\frac{\partial\Psi}{\partial X} = -V; \frac{\partial\Psi}{\partial Y} = U \quad (13)$$

$$\frac{\partial^2\Psi}{\partial X^2} + \frac{\partial^2\Psi}{\partial Y^2} = \left(\frac{\partial U}{\partial Y} - \frac{\partial V}{\partial X} \right) \quad (14)$$

Local and average Nusselt number along the hot bottom wall are calculated in the next equations [18]:

$$Nu_{loc} = -\frac{k_{na}}{k_{bf}} \left(\frac{\partial\theta}{\partial Y} \right)_{Y=0} \quad (15)$$

$$Nu_{ave} = \int_0^1 Nu_{loc} dX \quad (16)$$

3. Numerical Methodology, Grid Test and Code Validation

It is un-avoided to resolve the equations continuity, momentum and energy partial differential equations by a numerical method. For this reason, the dimensionless equations (1-4) and accompanying boundary conditions have been solved numerically with assistance of Galerkin finite element method (GFEM). P2-P1 Lagrange finite element is utilized to solve the continuity and momentum equations, and Lagrange-quadratic finite element is selected for energy equation.

In this study, the grid independency test has been examined for investigating the effect of two baffles on MHD natural convection in U-shaped superposed by nanofluid. The parameter value set for this test is AR=0.4, Ra=10⁶, $\lambda=0.52$, $\phi=0.05$, Ha=60 and $\nu=90^\circ$. The grid independency test evaluated for both average Nusselt number and maximum streamfunction since these results represented global variable. Also the gradient of this result are evaluated also which represent the percentage error. Five various cases of mesh size were tested as can see in table 3. It is found that grid size 150*150 was optimized for the results of the present work. To prove the accuracy of the current physical model, validation of calculating results is fulfilled by examining at the results constructed by the current code with the existing study. Thus, the implementation of the current code has been legalized successfully with new published work authorized by Ma et.al. [1]. For isotherms, streamlines and average Nusselt number, as depicted in figure 2 and table 4. Good comparison can noticed for all results.



4. Results and Discussion

In this section the results of the Fe₃O₄ nanofluid (with Table 1 properties) modeling in a U-shaped geometry as depicted in Fig. 1A including two cold baffles are discussed. As mentioned above, the bottom wall is in variable function temperature and the geometry is under the magnetic field effect in different angles. After the mesh generation as depicted in Fig. 1B, which is based on Table 3 confirmation for 150×150 grid numbers, the first results are depicted for the geometry with one baffle based on Yuan Ma et al. [1] to investigate the accuracy of results. As observed in Fig. 2 and Table 4 for the Ra=1e5, Φ=0.05, Ha=20, AR=0.4, the results are in excellent agreements for isothermline values, streamline shapes and the average Nusselt numbers. The maximum error of the applied method compared to the Yuan Ma et al. study is 1.244% in different Ha numbers.

Fig. 3 which is depicted for the streamlines and isotherms contours shows the effect of Hartmann number and aspect ratio (AR) number. By increasing the AR, the length of fins (cold walls) are much greater than the smaller AR and causes smaller area below the region of the cavity. So, the wide reason of higher temperature will be smaller in greater AR. Also, the vortexes in large AR are more complicated due to the geometry affected by the baffles. Furthermore, this figure confirms that by increasing the Ha number, vortexes separation will be appearing and the temperature distributions were approximately decreased in the whole regions especially near the upper walls.

Fig. 4 demonstrates the effect of AR and different nanoparticle shapes (Platelet and spherical shapes) on isotherm and streamlines. This figure confirms that ψ_{max} for platelet nanoparticles are greater than spherical shapes ($\lambda=1$), also the minimum value of stream value for platelet shapes is smaller than spherical shapes for all the ARs. From this figure, it can be concluded that AR=0.4 has the maximum ψ among the other examined aspect ratios.

The effect of magnetic field angle and Hartmann number on the average Nusselt number is presented via Fig. 5. Increasing the Hartmann number make a reduction on the average Nusselt number due to the magnetic effect on the Fe₃O₄ nanoparticles treatments, while increasing the inclination angle enhanced the heat transfer process as well as the average Nusselt numbers.

Fig. 6 which is obtained for the platelet nanoparticles when $\lambda = 0.52, \phi=0.05, \gamma=90^\circ$, illustrates the effect of Rayleigh and AR numbers on the average Nusselt number. Increasing both AR and Ra numbers enhanced heat transfer process and improved the average Nusselt numbers. Furthermore, no effect can be seen for non-magnetic (Ha=0) and low magnetic (Ha=20) from Fig. 6. This behavior of AR and Ha effects on Nu number is also presented in Fig. 7. Also, Fig. 7 says that increasing the nanoparticle volume fraction is an efficient method for increasing the average Nusselt number. Increasing the Ha, reduced the Nu which is due to negative effect of magnetic field on the nanoparticles motion (especially Brownian motion) which leads to lower heat transfer in higher Hartmann numbers. Finally, the effect of nanoparticles shape on the average Nusselt number is depicted in Fig. 8. As seen platelet, cylindrical, brick and spherical shapes have the maximum Nusselt numbers in sequence due to their physical effect on thermal conductivity based on Eq. 10. Also, AR=0.4 has the maximum values of Nusselt numbers among other values which can be introduced as the optimum AR in this application.

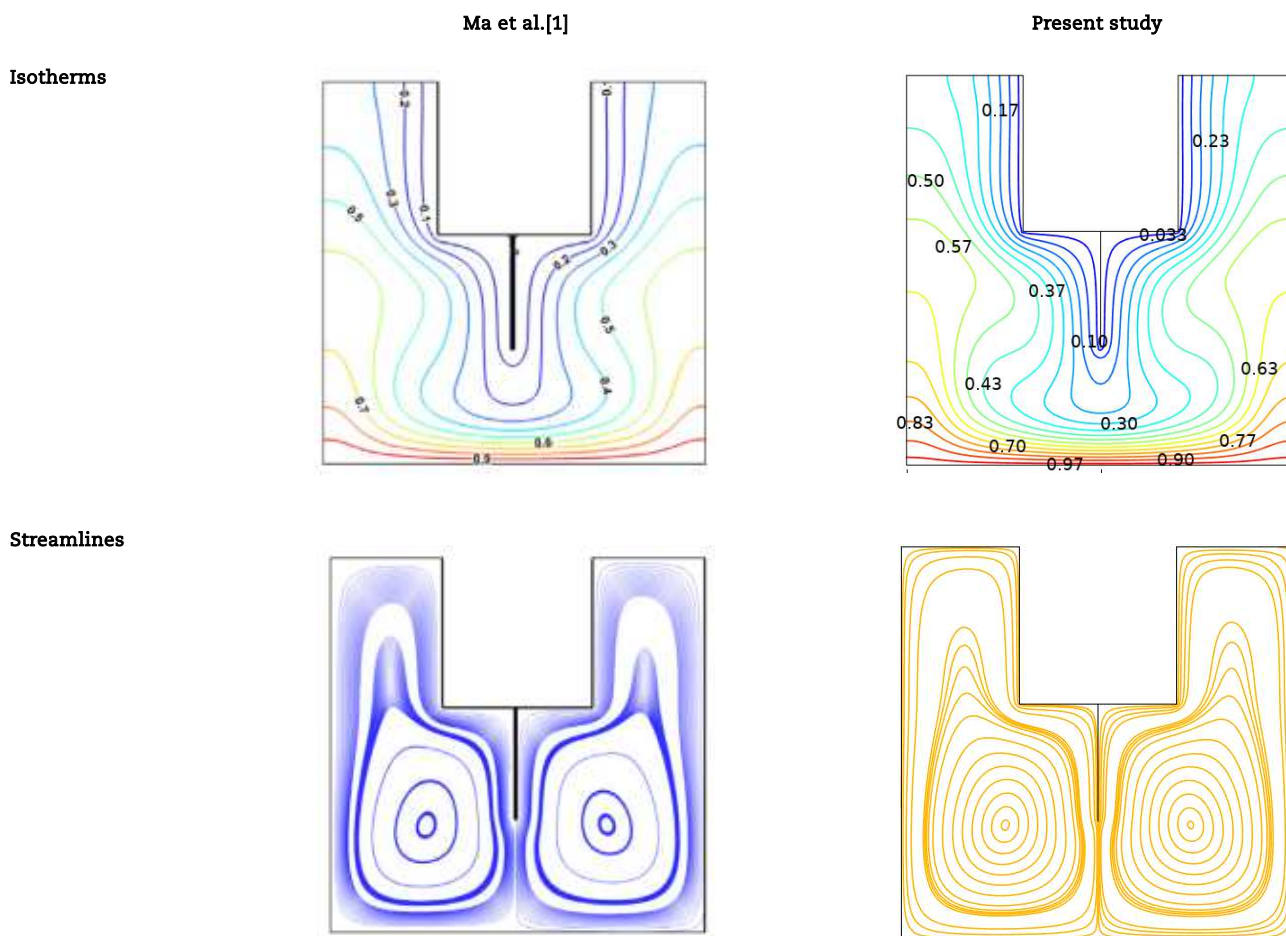


Fig. 2. Isotherms (upper row) and Streamlines (lower row) for Ra=10⁵, $\phi=0.05, Ha=20, AR=0.4$, present study and Yuan Ma et al. [1]



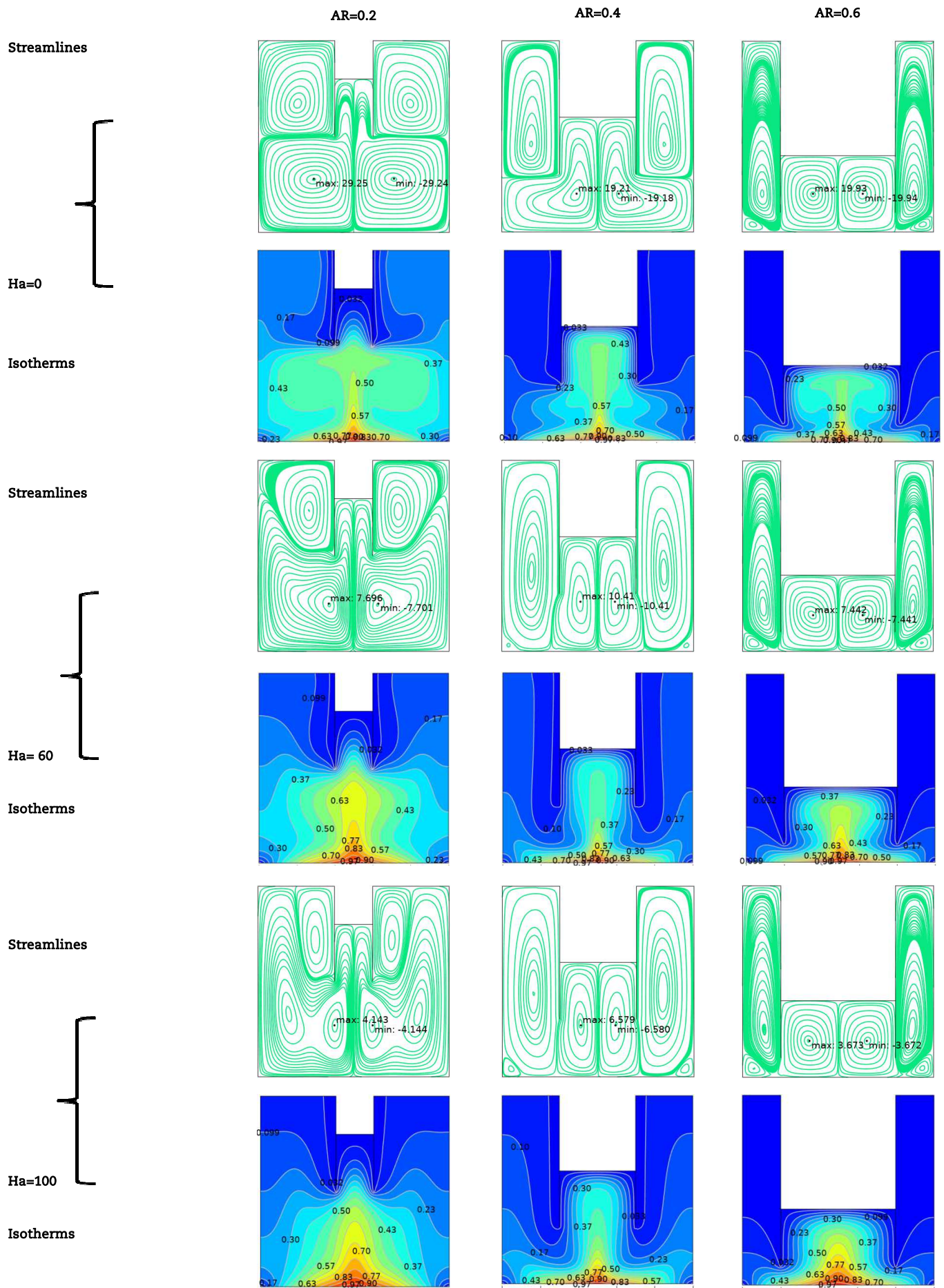


Fig. 3. Streamlines and Isotherms for different Aspect ratio, different Hartman number, $\lambda = 0.52$, $\phi = 0.05$, $Ra = 106$, $\gamma = 90$.



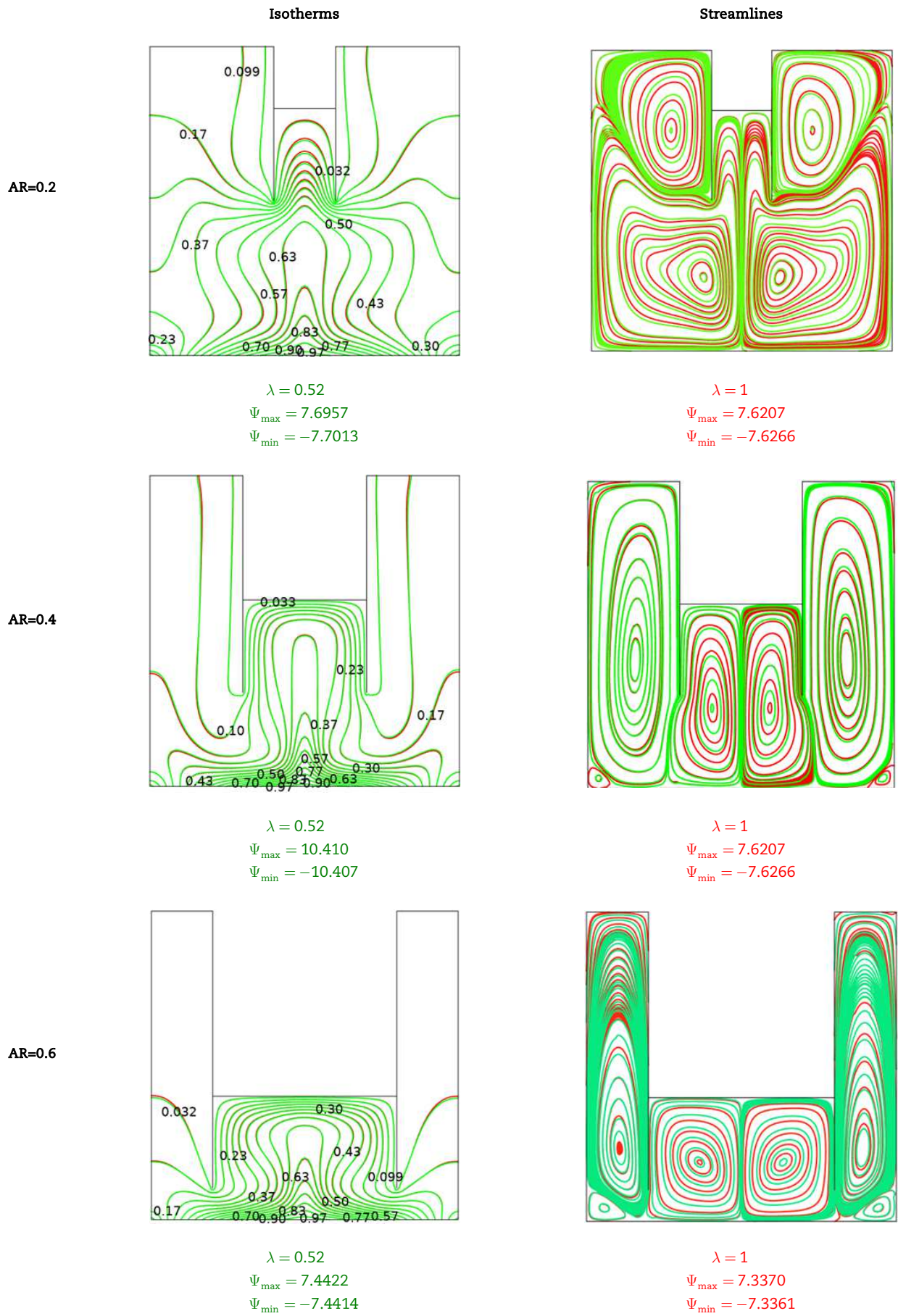


Fig. 4. Streamlines and Isotherms for different Aspect ratio, different Hartman number, $\phi=0.05$, $Ra=10^6$, $\gamma=90^\circ$



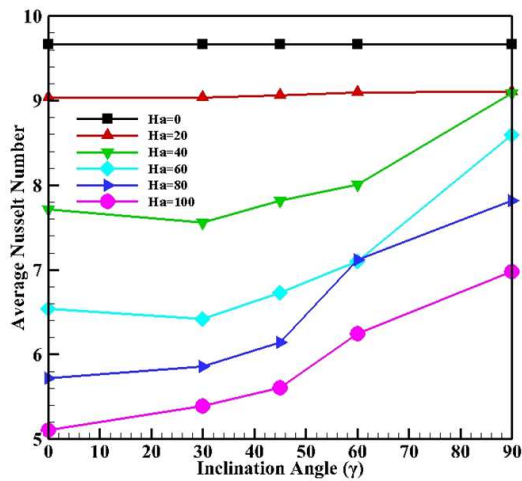


Fig. 5. Average Nusselt number for different angle of magnetic field and different Hartman number at $\lambda = 0.52, \varphi=0.05, Ra=10^6, AR=0.4$.

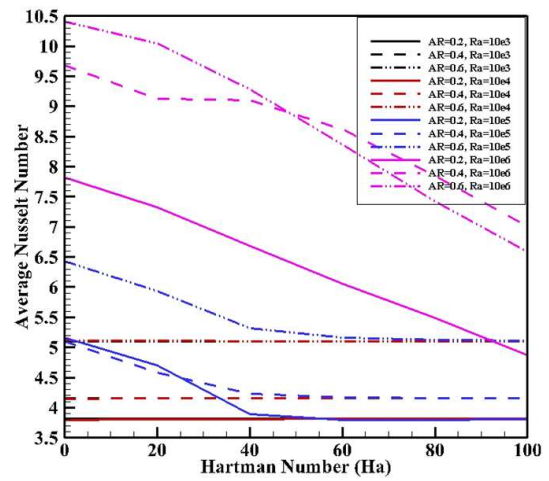


Fig. 6. Average Nusselt number with Hartman number for different Aspect ratio and Rayleigh number at $\lambda = 0.52, \varphi=0.05, \gamma=90^\circ$.

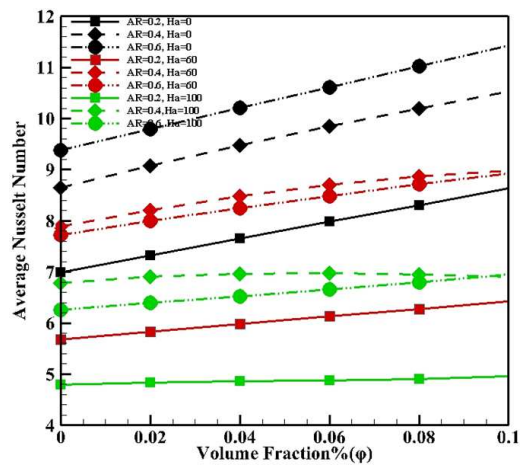


Fig. 7. Average Nusselt number with volume fraction for different Aspect ratio and Hartman number at $\lambda = 0.52, \varphi=0.05, \gamma=90^\circ$

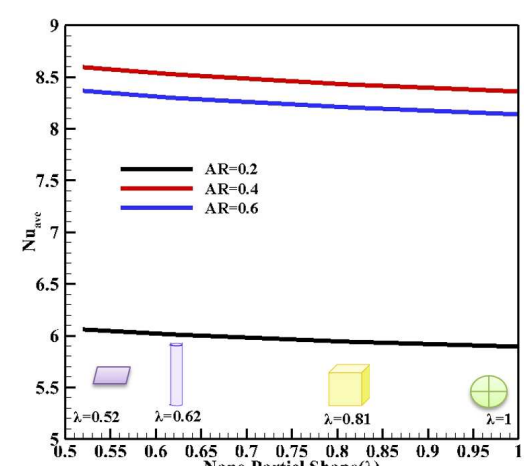


Fig. 8. Average Nusselt number with nanoparticle shape for different Aspect ratio at $\varphi=0.05, Ha=60, Ra=10^6, \gamma=90^\circ$

5. Conclusions

In this paper, natural convection heat transfer of U-shaped and nanofluid-filled cavity was studied numerically using the Galerkin weighted residual finite element method. The enclosure has two baffles and under the magnetic field with various inclination angle. The influence of Rayleigh number, Hartmann number, nanoparticles volume fraction, Aspect Ratio and shapes of nanoparticles on the heat transfer mechanism is investigated and it is found that Rayleigh number increment enhance the heat transfer process as well as the nanoparticles volume fraction. Also, it is found that $AR=0.4$ and platelet Fe_3O_4 nanoparticles had maximum Nusselt numbers for the heat transfer.

Author Contributions

H.K. Hamzah and F.H. Ali planned the scheme, initiated the project and solved the numerical code together at University of Babylon; M. Hatami and D. Jing analyzed the results; developed the mathematical modeling and examined the theory validation, also they provided suitable equations. The manuscript was written through the contribution of all authors in each related section. All authors discussed the results, reviewed and approved the final version of the manuscript.

Conflict of Interest

The authors declared no potential conflicts of interest with respect to the research, authorship and publication of this article.

Funding

M. Hatami received a partial financial support for this research, as a research plan at Esfarayen University of Technology. Also, D. Jing gratefully acknowledge the general financial grant from the National Natural Science Foundation of China (No.51776165), China Postdoctoral Science Foundation (No. 2017M610638) and Shaanxi Provincial Postdoctoral Funds (2017BSHYDZZ16).



Nomenclature

Symbol	Description	Unit
c_p	Heat capacitance	J/ kg. °C
Da	Darcy number	
g	Gravitational acceleration	m/s ²
k	Thermal conductivity of the fluid	W / m. °C
L	Height and width of the trapezoidal enclosure	m
Nu	Nusselt number	
N	Number of undulations	
P	Dimensionless pressure	
p	Pressure	N/m ²
Pr	Prandtl number	
r	Radius of the inner cylinder	m
R	Dimensionless radius of the inner cylinder	
Ra	Rayleigh number	
Re	Reynolds number	
Ri	Richardson number	
S	Porous layer thickness	m
T	Temperature	°C
U	Dimensionless velocity component in x-direction	
u	Dimensional velocity component in x-direction	m/s
V	Dimensionless velocity component in y-direction	
v	Dimensional velocity component in y-direction	m/s
X	Dimensionless coordinate in horizontal direction	
x	Cartesian coordinate in horizontal direction	m
Y	Dimensionless coordinate in vertical direction	
y	Cartesian coordinate in vertical direction	m

Greek Symbols

α	Thermal diffusivity	m ² /s
β	Volumetric thermal expansion coefficient	K ⁻¹
θ	Dimensionless temperature distribution	
ϕ	Solid volume fraction	
Ω	Dimensionless angular rotational velocity	
ω	Angular rotational velocity	rad/s
ν	Kinematic viscosity	m ² /s
ρ	Density	kg/m ³
μ	Dynamic viscosity	kg./m.s
ψ	Dimensionless stream function	
λ	Nano Particle Shape	

Subscripts

ave	Average
bf	Base fluid
loc	Local
c	Cold
eff	Effective
h	Hot
Max	Maximum
Min	Minimum
na	Nano fluid
o	Center of enclosure
sp	Solid particles

References

- [1] Ma, Y., Mohebbi, R., Rashidi, M. M., Yang, Z., Sheremet, M. A., Numerical study of MHD nanofluid natural convection in a baffled U-shaped enclosure, *International Journal of Heat and Mass Transfer*, 130, 2019, 123-134.
- [2] Abedini, A., Armaghani, T., Chamkha, A. J., MHD free convection heat transfer of a water-Fe₃O₄ nanofluid in a baffled C-shaped enclosure, *Journal of Thermal Analysis and Calorimetry*, 135(1), 2019, 685-695.
- [3] Aghakhani, S., Pordanjani, A. H., Karimipour, A., Abdollahi, A., Afrand, M., Numerical investigation of heat transfer in a power-law non-Newtonian fluid in a C-Shaped cavity with magnetic field effect using finite difference lattice Boltzmann method, *Computers & Fluids*, 176, 2018, 51-67.
- [4] Hussain, S. H., Sabah, R., Hassan Ali, F., Numerical study of natural convection heat transfer of air flow inside a corrugated enclosure in the presence of an inclined heated plate, *Progress in Computational Fluid Dynamics, An International Journal*, 13(1), 2013, 34-43.
- [5] Hussain, S. H., Mohammed, R. N., Effects of out of phase and inclination angles on natural convection heat transfer flow of air inside a sinusoidal corrugated enclosure with spatially variable wall temperature, *Journal of Enhanced Heat Transfer*, 18(5), 2011, 403-417.
- [6] Ali, F. H., Numerical simulation of natural convection in an oblique enclosure filled with silver-water nanofluid, *Al-Qadisiyah Journal for Engineering Sciences*, 9(1), 2016, 87-105.
- [7] Abu-Nada, E., Oztop, H. F., Effects of inclination angle on natural convection in enclosures filled with Cu-water nanofluid, *International Journal of Heat and Fluid Flow*, 30(4), 2009, 669-678.
- [8] Abdulkadhim, A., Hamzah, H. K., Abed, M. A., Ali, H. F., Numerical study of entropy generation and natural convection heat transfer in trapezoidal enclosure with a thin baffle attached to inner wall using liquid nanofluid, In *Annales de Chimie Science des Materiaux*, 25(1-2), 2017, 7-28.
- [9] Mahian, O., Kianifar, A., Kleinstreuer, C., Moh'd A. A. N., Pop, I., Sahin, A. Z., Wongwises, S., A review of entropy generation in nanofluid flow, *International Journal of Heat and Mass Transfer*, 65, 2013, 514-532.
- [10] Hatami, M., Ganji, D. D., Motion of a spherical particle in a fluid forced vortex by DQM and DTM, *Particuology*, 16, 2014, 206-212.



- [11] Hatami, M., Ganji, D. D., Motion of a spherical particle on a rotating parabola using Lagrangian and high accuracy multi-step differential transformation method, *Powder Technology*, 258, 2014, 94-98.
- [12] Dogonchi, A. S., Hatami, M., Domairry, G., Motion analysis of a spherical solid particle in plane Couette Newtonian fluid flow, *Powder Technology*, 274, 2015, 186-192.
- [13] Hatami, M., Sheikholeslami, M., Domairry, G., High accuracy analysis for motion of a spherical particle in plane Couette fluid flow by multi-step differential transformation method, *Powder Technology*, 260, 2014, 59-67.
- [14] Ghadikolaei, S. S., Hosseinzadeh, K., Ganji, D. D., Hatami, M., Fe₃O₄-(CH₂OH)₂ nanofluid analysis in a porous medium under MHD radiative boundary layer and dusty fluid, *Journal of Molecular Liquids*, 258, 2018, 172-185.
- [15] Hatami, M., Song, D., Jing, D., Optimization of a circular-wavy cavity filled by nanofluid under the natural convection heat transfer condition, *International Journal of Heat and Mass Transfer*, 98, 2016, 758-767.
- [16] Hatami, M., Nanoparticles migration around the heated cylinder during the RSM optimization of a wavy-wall enclosure, *Advanced Powder Technology*, 28(3), 2017, 890-899.
- [17] Tang, W., Hatami, M., Zhou, J., Jing, D., Natural convection heat transfer in a nanofluid-filled cavity with double sinusoidal wavy walls of various phase deviations, *International Journal of Heat and Mass Transfer*, 115, 2017, 430-440.
- [18] Hatami, M., Jing, D., Optimization of wavy direct absorber solar collector (WDASC) using Al₂O₃-water nanofluid and RSM analysis, *Applied Thermal Engineering*, 121, 2017, 1040-1050.
- [19] Hatami, M., Zhou, J., Geng, J., Song, D., Jing, D., Optimization of a lid-driven T-shaped porous cavity to improve the nanofluids mixed convection heat transfer, *Journal of Molecular Liquids*, 231, 2017, 620-631.
- [20] Zhou, J., Hatami, M., Song, D., Jing, D., Design of microchannel heat sink with wavy channel and its time-efficient optimization with combined RSM and FVM methods, *International Journal of Heat and Mass Transfer*, 103, 2016, 715-724.
- [21] Kefayati, G. R., Simulation of heat transfer and entropy generation of MHD natural convection of non-Newtonian nanofluid in an enclosure, *International Journal of Heat and Mass Transfer*, 92, 2016, 1066-1089.
- [22] Kefayati, G. H. R., Double-diffusive natural convection and entropy generation of Bingham fluid in an inclined cavity, *International Journal of Heat and Mass Transfer*, 116, 2018, 762-812.
- [23] Kefayati, G. H. R., Tang, H., Simulation of natural convection and entropy generation of MHD non-Newtonian nanofluid in a cavity using Buongiorno's mathematical model, *International Journal of Hydrogen Energy*, 42(27), 2017, 17284-17327.
- [24] Menni, Y., Azzi, A., Chamkha, A. J., A review of solar energy collectors: models and applications, *Journal of Applied and Computational Mechanics*, 4(4), 2018, 375-401.
- [25] Kefayati, G. R., Magnetic field effect on heat and mass transfer of mixed convection of shear-thinning fluids in a lid-driven enclosure with non-uniform boundary conditions, *Journal of the Taiwan Institute of Chemical Engineers*, 51, 2015, 20-33.
- [26] Kefayati, G. R., Lattice Boltzmann simulation of natural convection in partially heated cavities utilizing kerosene/cobalt ferrofluid, *Iranian Journal of Science and Technology, Transactions of Electrical Engineering*, 37(M2), 2013, 107-118.
- [27] Kefayati, G. R., Mesoscopic simulation of magnetic field effect on natural convection of power-law fluids in a partially heated cavity, *Chemical Engineering Research and Design*, 94, 2015, 337-354.
- [28] Kefayati, G. R., Tang, H., MHD thermosolutal natural convection and entropy generation of Carreau fluid in a heated enclosure with two inner circular cold cylinders, using LBM, *International Journal of Heat and Mass Transfer*, 126, 2018, 508-530.
- [29] Mehryan, S. A. M., Izadi, M., Chamkha, A. J., Sheremet, M. A., Natural convection and entropy generation of a ferrofluid in a square enclosure under the effect of a horizontal periodic magnetic field, *Journal of Molecular Liquids*, 263, 2018, 510-525.
- [30] Dogonchi, A. S., Sheremet, M. A., Pop, I., Ganji, D. D., MHD natural convection of Cu/H₂O nanofluid in a horizontal semi-cylinder with a local triangular heater, *International Journal of Numerical Methods for Heat & Fluid Flow*, 28(12), 2018, 2979-2996.
- [31] Dogonchi, A. S., Sheremet, M. A., Ganji, D. D., Pop, I., Free convection of copper-water nanofluid in a porous gap between hot rectangular cylinder and cold circular cylinder under the effect of inclined magnetic field, *Journal of Thermal Analysis and Calorimetry*, 135(2), 2019, 1171-1184.
- [32] Shah, Z., Kumam, P., Deebani, W., Radiative MHD Casson Nanofluid Flow with Activation energy and chemical reaction over past nonlinearly stretching surface through Entropy generation, *Scientific Reports*, 10(1), 2020, 1-14.
- [33] Alsabery, A. I., Sheremet, M. A., Chamkha, A. J., Hashim, I.J.S.R., MHD convective heat transfer in a discretely heated square cavity with conductive inner block using two-phase nanofluid model, *Scientific Reports*, 8(1), 2018, 1-23.
- [34] Dinarvand, S., Rostami, M. N., Pop, I., A novel hybridity model for TiO₂-CuO/water hybrid nanofluid flow over a static/moving wedge or corner, *Scientific Reports*, 9(1), 2019, 1-11.
- [35] Alsabery, A. I., Chamkha, A. J., Saleh, H., Hashim, I., Natural convection flow of a nanofluid in an inclined square enclosure partially filled with a porous medium, *Scientific Reports*, 7(1), 2017, 1-18.
- [36] Hamilton R.L., Crosser O.K., Thermal conductivity of heterogeneous two component systems, *Industrial & Engineering Chemistry Fundamentals*, 1(3), 1962, 187-91.

ORCID iD

Hameed K. Hamzah  <https://orcid.org/0000-0003-0983-4776>

Farooq H. Ali  <https://orcid.org/0000-0003-0082-3261>

M. Hatami  <https://orcid.org/0000-0001-5657-6445>

D. Jing  <https://orcid.org/0000-0001-6062-9239>



© 2020 by the authors. Licensee SCU, Ahvaz, Iran. This article is an open access article distributed under the terms and conditions of the Creative Commons Attribution-NonCommercial 4.0 International (CC BY-NC 4.0 license) (<http://creativecommons.org/licenses/by-nc/4.0/>).

How to cite this article: Hamzah H.K., Ali F.A., Hatami M., Jing D. Effect of Two Baffles on MHD Natural Convection in U-Shape Superposed by Solid Nanoparticle having Different Shapes, *J. Appl. Comput. Mech.*, 6(SI), 2020, 1200-1209. <https://doi.org/10.22055/JACM.2020.33064.2141>

